THE INTERFACIAL MASS DETECTION WITH LAMB-WAVE SENSORS

Junru Wu
Department of Physics, University of Vermont
Burlington, VT 05405

Zhemin Zhu
Institute of Acoustics, Nanjing University
The People's Republic of China

INTRODUCTION

A sensor which measures physical parameters of a liquid with high sensitivity and accuracy is in great demand in medicine, biology, chemistry and environmental science [1]. Recently, resurgent interest in Lamb waves was initiated in their applications of multisensors [2]. The principle of these Lamb-Wave Sensors is that the propagation velocity of Lamb waves changes when a plate is bordered with a liquid. In this paper, we report the results of our recent theoretical investigations of the effects of bordering liquid layers on the propagation of Lamb waves in a solid plate.

We devote the first part of the paper to the derivation of dispersion relations of Lamb waves in a plate bordered with layers of a liquid at its both sides. Numerical solutions of the dispersion equations are presented in the second part. For very thin plates that is of interest of biosensing applications, the numerical results are compared with those derived from a treatment using concept of acoustic impedance of bending waves. We show that the acoustic impedance approach is an good approximation for a thin plate. We also show that for the case when a thin plate is in contact with a liquid layer at one side, the acoustic impedance approach is appropriate.

DISPERSION EQUATIONS

The configuration of the case for investigation is as follows: A solid isotropic plate of thickness 2d extends to infinity in both the x and y directions (Fig. 1). It is bordered on both the top and the bottom sides of the plate with an infinitely large layer of homogeneous liquid of thickness, h. A harmonic Lamb wave propagates along the x direction. The displacement potential functions of longitudinal waves and shear waves in solid, ϕ_S and Ψ_S, are used to describe wave propagation in a plate. The x and z components of the displacement, u_s and w_s, respectively, are given by $u_S = \partial\phi_S/\partial x - \partial\Psi_S/\partial z$ and $w_S = \partial\phi_S/\partial z + \partial\Psi_S/\partial x$ [3]. The

Review of Progress in Quantitative Nondestructive Evaluation, Vol. 11
Edited by D.O. Thompson and D.E. Chimenti, Plenum Press, New York, 1992

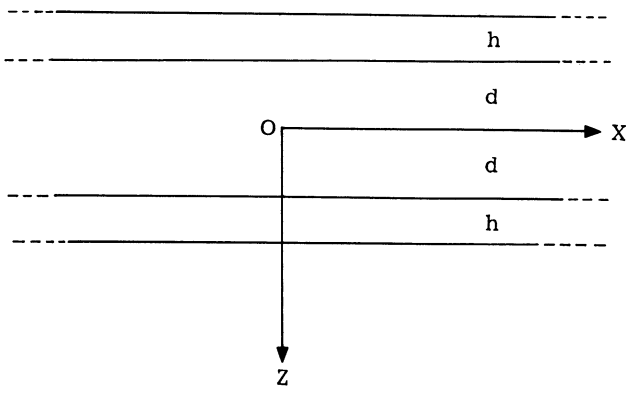

Fig. 1. Illustration of the coordinate system used.

displacement potential functions of ϕ_{L1} and ϕ_{L2} are used for the same purpose for the top and the bottom parts of the liquids respectively, i. e. $u_{Li} = \partial\phi_{Li}/\partial x$, $w_{Li} = \partial\phi_{Li}/\partial z$ (i = 1 for the top liquid and i = 2 for the bottom liquid). For an ideal liquid, they all observe the so-called the Helmholtz equation as follows:

$$\begin{aligned} &\nabla^2\phi_S + k_l^2\phi_S = 0, \\ &\nabla^2\Psi_S + k_t^2\Psi_S = 0, \\ &\nabla^2\phi_{L1} + k_L^2\phi_{L1} = 0, \\ &\nabla^2\phi_{L2} + k_L^2\phi_{L2} = 0, \end{aligned} \qquad (1)$$

where $k_l = \omega/c_l$, $k_t = \omega/c_t$, $k_L = \omega/c_L$, ω is the angular frequency, c_l, c_t, and c_L are the speeds of the longitudinal waves in the solid, transverse waves in the solid and the speed of sound in the liquid respectively. We now seek the harmonic travelling-wave (in x direction) solutions of equation 1 as

$$\begin{aligned} &\phi_S = [A_s\cosh(qz) + B_a\sinh(qz)]\exp[i(\omega t - kx)] \text{ for } (-d \le z \le d), \\ &\Psi_S = [D_s\sinh(sz) + C_a\cosh(sz)]\exp[i(\omega t - kx)] \text{ for } (-d \le z \le d), \\ &\phi_{L1} = A_1\sin\{\gamma[z - (d + h)]\}\exp[i(\omega t - kx)] \text{ for } [d \le z \le (d + h)], \\ &\phi_{L2} = A_2\sin\{\gamma[z + (d + h)]\}\exp[i(\omega t - kx)] \text{ for } [-(d + h) \le z \le -d], \end{aligned} \qquad (2)$$

where k is the wave number of the travelling waves, $q = (k^2 - k_l^2)^{1/2}$, $s = (k^2 - k_t^2)^{1/2}$, and $\gamma = (k_L^2 - k^2)^{1/2}$. The main difference between this case and the case of Leaky Lamb waves is that the functions ϕ_{L1} and ϕ_{L2} here are chosen in such a way that the acoustical pressure is zero at $z = \pm (d + h)$; in other words, ϕ_{L1} and ϕ_{L2} here are of standing waves solutions, for Leaky Lamb waves they are of travelling waves. The wave number k is to be determined by satisfying the following boundary conditions. At the solid-liquid interfaces ($z = \pm d$): 1. the magnitude of the normal component of the stress tensor of the plate, $\sigma_{zz} = \lambda(\partial^2\phi_S/\partial x^2 + \partial^2\phi_S/\partial z^2) + 2\mu(\partial^2\phi_S/\partial z^2 + \partial^2\Psi_S/\partial x\partial z)$, where λ and μ are the elastic Lamé constants, should be equal to the pressure of the liquid; 2. the tangential component of the stress tensor, $\sigma_{xz} = \mu(2\partial^2\phi_S/\partial x\partial z + \partial^2\Psi_S/\partial x^2 - \partial^2\Psi_S/\partial z^2)$, should be zero; 3. the normal component of the displacement of the solid, $w_S = (\partial\phi_S/\partial z + \partial\Psi_S/\partial x)$, should be equal to that of liquid there, $w_L = (\partial\phi_L/\partial z)$. Note that $c_l = [(\lambda + 2\mu)/\rho_S]^{1/2}$ (ρ_S and ρ_L, which will appear later, are the densities of the solid and the liquid respectively) and $c_t =$

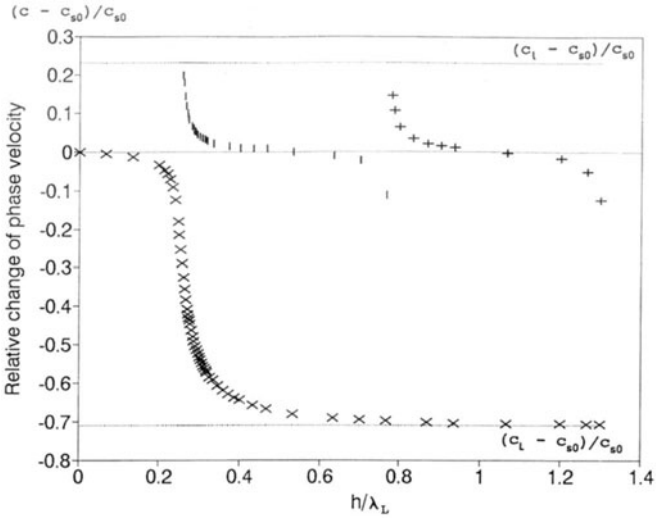

Fig.2. Plots of the numerical solutions of the relative phase velocity change, $(c - c_{s0})/c_{s0}$, vs h/λ_L from Eq. 4 for S_0 mode (1 MHz) in the presence of water layers on two sides of the aluminum plate of thickness 0.0954 cm.

$(\mu/\rho_S)^{1/2}$, the following set of equations should be satisfied:

$$\begin{aligned}
&\rho_S[\partial^2\phi_S/\partial t^2 - 2c_t^2(\partial^2\phi_S/\partial x^2 - \partial^2\Psi_S/\partial x\partial z)]\|_{z=\pm d} = -\omega^2\rho_L\phi_{L1(2)}|_{z=\pm d}, \\
&(\partial^2\Psi_S/\partial z^2 - \partial^2\Psi_S/\partial x^2 - 2\partial^2\phi_S/\partial x\partial z)|_{z=\pm d} = 0, \\
&(\partial\phi_S/\partial z + \partial\Psi_S/\partial x)|_{z=\pm d} = \partial\phi_{L1(2)}/\partial z|_{z=\pm d}.
\end{aligned} \tag{3}$$

Substituting Eq. 2 into Eq. 3 and after some algebraic manipulations of the determinant, the conditions of $\gamma \neq 0$ and $\gamma h \neq (2n + 1)\pi/2$, n = 0, 1 , 2 ... lead to the following two equations:

$$(k^2 + s^2)^2\coth(qd) - 4k^2qs\coth(sd) = -(\rho_L/\rho_S)k_t^4q\tan(\gamma h)/\gamma, \tag{4}$$

$$(k^2 + s^2)^2\tanh(qd) - 4k^2qs\tanh(sd) = -(\rho_L/\rho_S)k_t^4q\tan(\gamma h)/\gamma. \tag{5}$$

If we let ρ_L approach zero, Eqs. 4 and 5 recover the dispersion equations for Lamb waves of free boundaries [3]. If we let d approach infinity, Eqs. 4 and 5 become the dispersion equations for Rayleigh waves in the case of an infinite half-spaced solid bordered with a liquid layer of finite thickness[3].

Like the Lamb waves of free boundary cases, when k is determined by Eq. 4, the waves may be called symmetrical Lamb waves (S modes) ; when k is determined by Eq. 5, the waves may be called antisymmetrical Lamb waves (A modes).

One observation of the dispersion equations is that h, the thickness of the liquid layer on the right sides of the equations, is a parameter of the periodic tangent function. This reflects the periodic nature of the influence due to the presence of the liquid layers of varying thickness which has been confirmed by our numerical calculations discussed in the next section.

NUMERICAL CALCULATIONS

For a particular mode of Lamb waves, we may solve for k numerically in equations 4 and 5 for various h. From the value of k, we may then calculate the phase velocity c, which is equal to ω/k, for the particular h. Since the lowest symmetrical mode S_0 and antisymmetrical mode A_0 are most commonly used in sensor applications, we solve the cases of S_0 and A_0 modes for plates of the different thickness.

A Plate of Medium Thickness

A plate thickness is such that $k_t d \approx 1$. For the calculations followed, frequency is set equal to 1 MHz, the speed of sound in water, $c_L = 1.5 \times 10^5$ cm/s, the wavelength of the sound waves in water of the frequency $\lambda_L = 0.15$ cm, the thickness of the aluminum plate, $2d = 0.954$ mm, c_l, c_t, the phase velocity of S_0 mode, c_{s0}, and the phase velocity of A_0 mode, c_{a0}, at the frequency and thickness are, respectively, equal to 6.4×10^5, 3.0×10^5, 5.250×10^5 cm/s, and 2.30×10^5.

Figure 2 contains a plot of the numerical results of the relative change of the phase velocity for the aluminum plate, $(c - c_{s0})/c_{s0}$, vs the ratio of the thickness of water to the wavelength of acoustic waves in water, h/λ_L, where c is the phase velocity when there is water layers present. One observation of the plot is that the value of $(c - c_{s0})/c_{s0}$ decreasingly approaches $(c_L - c_{s0})/c_{s0}$ as h/λ_L increases from 0. When h/λ_L just passes $0.25\lambda_L$ from the left, the second branch of $(c - c_{s0})/c_{s0}$ appears. The value of $(c - c_{s0})/c_{s0}$ of the second branch decreases from a value very close to $(c_l - c_{s0})/c_{s0}$ until h/λ_L reaches 0.78. Then, the third branch appears. The third branch looks similar with the second one. The ranges of h/λ_L both for the second and third branches are approximately equal to 0.5. This kind of process repeats; more branches emerge as h/λ_L keeps increasing. Notice that when $h/\lambda_L = (2n + 1)/4$, where $n = 0,1,2...$, the values of the thickness of water, h, happen to satisfy the conditions of the acoustic modes along z direction for a liquid layer which is free on the top and fixed on the bottom.

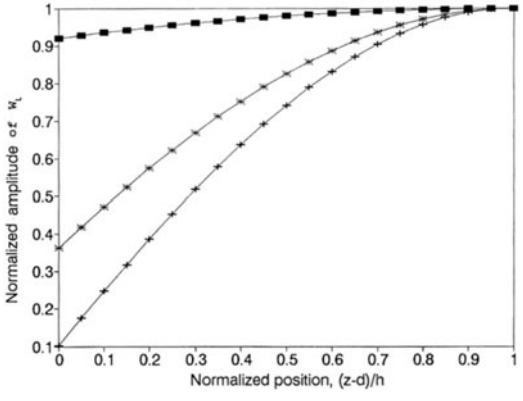

Fig.3. Plots of the particle velocity amplitude of water, $W_L(z)/W_L(h+d)$, vs $(z-d)/h$. Three curves from the top to the bottom correspond respectively to $h/\lambda_L = 0.067$, 0.20, and 0.25 of the first branch.

To understand the physics of these branches, we plot the normalized displacement amplitude of water, $W_L(z)/W_L(d+h)$, vs the vertical position in the liquid for different h/λ_L. Incidentally, these curves shown in Fig. 3 could only be used to compare the amplitude at different z on the same curve for the same h/λ_L and should not be used to compare the amplitudes between the different curves corresponding to different h/λ_L. Figure 3 contains three curves corresponding to three different h for the first branch; from the top to the bottom, h/λ_L = 0.067, 0.20, 0.25 respectively. Notice the first mode of the liquid gradually developed as h/λ_L increases from 0 to 0.25. It can easily shown the second mode of the liquid gradually developed within the range of the liquid thickness corresponding to the second branch, and so on.

Figure 4 is a plot which shows relative phase velocity change of A_0 mode for the same situation of S_0 mode shown in Fig. (2). Note that the second and third branches emerge at h/λ_L = 0.34, 0.92 respectively.

A Thin Plate

A plate is thin when $k_t d << 1$. This is a regime that is of great interest for biosensing. We have calculated the relative change both for the phase velocity of A_0 and S_0 modes for two different cases. The first one is for an aluminum plate of thickness of 50 μm; frequency is 1 MHz, thus $k_t d \approx 0.1$. The other parameters are the same as before. The symbols of "+" in Fig. 5 are the numerical results calculated from the dispersion equations, which show that the relative phase velocity, $(c - c_{a0})/c_{a0}$, is a decreasing function of $h/(2d)$. For the interest of practical applications we do not include the results of the cases when $h/(2d) > 2$.

The second case is for an thin Zinc Oxide (ZnO) film of thickness of 3.0 μm that is widely used for biosensors [2]. For this case $\rho_s = 5.68 \times 10^3$ kg/m^3, $c_l = 6.4 \times 10^5$ cm/s,

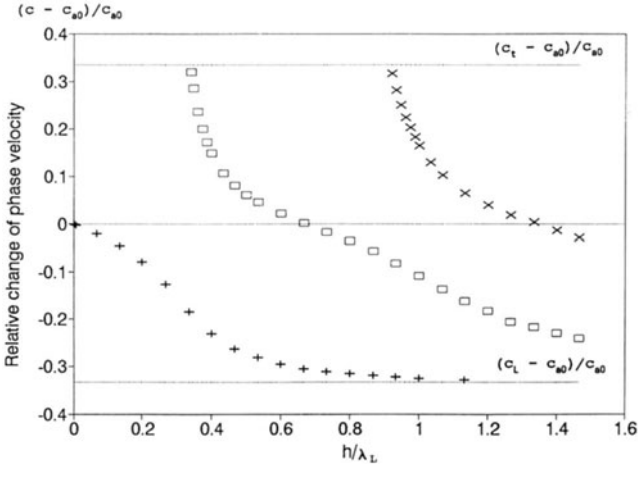

Fig.4. A plot of the relative phase velocity change of A_0 mode for the same situation of Fig. 2.

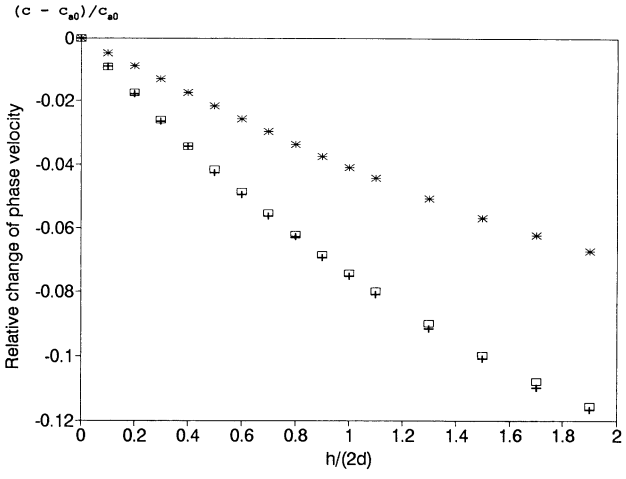

Fig.5. The relative phase velocity change vs h/(2d) for the case of $k_t d \approx 0.1$. The symbols of "+" represent the results calculated from the dispersion equations when both sides of the plate are bordered with a water layer, the symbols of the empty rectangles stand for the results calculated from the acoustic impedance approach for the same situation, and the symbols of "*" represent the results derived from the acoustic impedance approach when only one side of the plate is bordered with a water layer.

$c_t = 2.945 \times 10^5$ cm/s, frequency = 4.7 MHz. Thus $k_t d \approx 0.015$. The symbols of "+" in Fig. 6 represent the numerical results of the relative change of the phase velocity calculated from the dispersion equations. Compared Fig. 6 with Fig. 5, in the range between 0 and 2.0 for h/(2d), the relative changes of the phase velocity look very similar for these two cases. Notice that the horizontal axis in both cases is h/(2d) and d is different for these two cases. Therefore, to achieve the same amount of the relative phase velocity change, it needs thicker water layer for thick plate than the thin plate.

As far as S_0 mode is concerned, for these two cases, it is found that the relative changes of the phase velocity is negligible. This, in fact, suggests that S_0 mode of thin plate is not a good choice for biosensing regarding to applications of this principle.

For cases of $k_t d << 1$, S_0 mode becomes dispersionless; the phase velocity is equal to the group velocity and equal to $\{E/[\rho_s(1 - \upsilon^2)]\}^{1/2}$, where E is Young's modulus and υ is Poisson's ratio. A_0 mode, meanwhile, becomes the flexural or bending wave of the plate; its phase velocity, c_{a0}, is approximately equal to $(\omega d)^{1/2}\{E/[3(1 - \upsilon^2)\rho_s]\}^{1/4}$, and its group velocity, c_{ga0} is equal to $2c_{a0}$. For a thin plate, A_0 mode is essentially a transverse mode, i. e. the z-component of the displacement, W_z, dominates. We plot W_z for the A_0 mode vs z/d for these three cases shown in Fig. 7. Curve A, B, and C are respectively for the cases of $k_t d \approx 0.015$, 0.1, and 1. One obvious observation is that W_z is more or less constant with respect to z for thin plates. Under such circumstance, the plate may be considered as a lump element

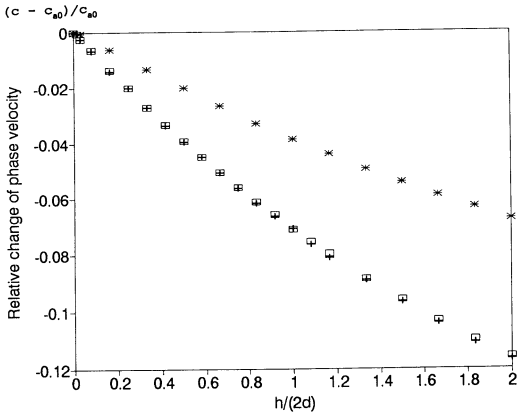

Fig.6. The relative phase velocity change vs h/(2d) for the case of $k_t d \approx 0.015$. The symbols of "+" represent the results calculated from the dispersion equations when both sides of the plate are bordered with a water layer, the symbols of the empty rectangles stand for the results calculated from the acoustic impedance approach for the same situation, and the symbols of "*" represent the results derived from the acoustic impedance approach when only one side of the plate is bordered with a water layer.

instead of a distributed system. In other words, the acoustic impedance concept could be used as a good approximation. For bending waves, the acoustic impedance of the plate, Z_s, is given by [4, 5]

$$Z_s = i\omega M - iBk^4/\omega, \qquad (6)$$

where M is the mass per unit area of the plate, which is equal to $\rho_s(2d)$, B is its bending stiffness, which is given by $[E/(1 - \upsilon^2)](2d^3/3)$. Meanwhile, the acoustic impedance of the water layer seen by the plate, Z_L, may be calculated from the acoustic pressure of the plate divided by the z-component of the particle velocity at the surface of the plate, which is

$$Z_L = i\rho_L\omega\tan(\gamma h)/\gamma. \qquad (7)$$

When the plate and the fluid layers are coupled together, the total acoustic impedance of the system, Z_t, is simply equal to the equivalent acoustic impedance of Z_s and two of Z_L in series, i. e. $Z_t = Z_s + 2Z_L$. Since the total impedance of the system, Z_t, is pure imaginary (any irreversible loss is neglected), the phase velocity of this case can be determined under the condition $Z_t = 0$ [4], which yields

$$M - Bk^4/\omega^2 = -2\rho_L\tan(\gamma h)/\gamma. \qquad (8)$$

The numerical results calculated from the equation for the above-mentioned thin plate cases are plotted in Fig. 5 and Fig. 6 by empty rectangles. We could see the results are in excellent agreement with those derived from the dispersion equations. However, they are in better agreement for the lower $k_t d$ case shown in Fig. 6 than the higher case shown in Fig. 5. In order to see the limitation of the acoustic

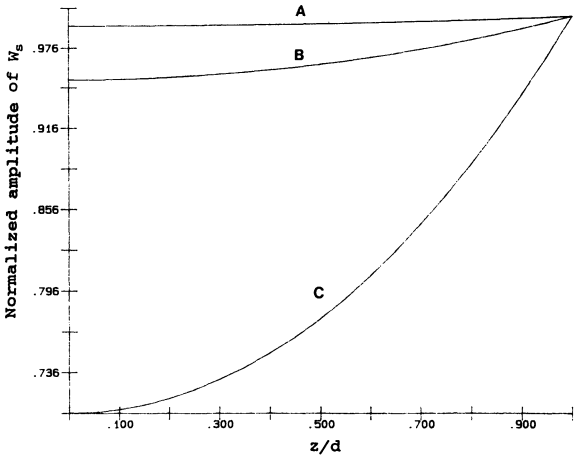

Fig.7. Plots of the amplitude of the z-component of the particle velocity of A_0 mode, W_z, vs z/d. Curve A, B, and C are respectively for the cases of $k_t d \approx 0.015$, 0.1, and 1.

impedance approach, we also compared the two approaches for the $k_t d \approx 1$ (d = 0.0477 cm) case. For this case, the maximum relative error caused by using the acoustic impedance approach reaches 16%. This is probably what we would expect from Fig. 7. Curve C in Fig. 7 describes the amplitude of the particle velocity of A_0 mode of the plate vs z/d for the case of $k_t d \approx 1$. At the center of plate, the amplitude is only about 70% of that at the surface of the plate. Therefore, it is not a good approximation to consider the plate as a lump element.

For applications of biosensing, it is useful to consider situations when a thin plate is bordered with a liquid layer on one side and the other side is free. For thin plates, as we have shown that the acoustic impedance approach is a valid one. Now the total impedance is the sum of Z_s and Z_L. The phase velocity can be determined by letting $Z_s + Z_L = 0$. The results derived from the equation for the above-described thin plate cases are represented by "*" in Figs. 5 and 6.

ACKNOWLEDGEMENT

This work is partially supported by BF Goodrich Simmonds Precision Aircraft System.

REFERENCES

1. M. D. Ward, and D. A. Buttry, Sciences, 249, 1000 (1990).
2. S. W. Wenzel, and R. M. White, IEEE Transactions on Electron Devices 35, 735 (1988).
3. I. A. Viktorov, Rayleigh and Lamb waves, physical theory and applications (Plenum Press, New York, 1967).
4. G. Kurtze, and R. H. Bolt, Acustica 9, 238 (1959).
5. P. M. Morse, Vibration and Sound (the American Institute of Physics for the Acoustical Society of America, 1976).